The Thesis Committee for Jarred David Canning
certifies that this is the approved version of the following thesis:

Long-Term Reliability Analysis of Wave Energy Converters

APPROVED BY
SUPERVISING COMMITTEE:

Lance Manuel, Supervisor

Spyros A. Kinnas

Long-Term Reliability Analysis of Wave Energy Converters

by

Jarred David Canning

THESIS

Presented to the Faculty of the Graduate School of

The University of Texas at Austin

in Partial Fulfillment

of the Requirements

for the Degree of

Master of Science in Engineering

THE UNIVERSITY OF TEXAS AT AUSTIN

December 2017

Dedicated to my parents and siblings

Acknowledgments

To my advisor, teacher, and role-model, Dr. Lance Manuel. I am very happy to have continued my education under your supervision. You were always helpful, supportive, and strict when need be. I enjoyed our talks and classes together as we came to know one another.

I am thankful for Ryan Coe, who brought me onto this project and guided my work. Thank you for taking a chance on me and helping me develop as a student and a person. Your advice and leadership are invaluable.

I am grateful to Phong Nguyen, who was instrumental throughout our research. I am very happy to have had the chance to work alongside you in this project and learn from your methods.

A special mention to Aubrey Eckert-Gallup, Nevin Martin, and Carlos Michelén. Thank you all for being open and receptive to my questions in addition to leading the research efforts. Your help is much appreciated.

I am also grateful to the following university faculty: Spyros Kinnas, Loukas Kallivokas, and John F. Burgin for their supportive and motivating teaching abilities. I thoroughly enjoyed taking your courses.

To the interns and MUSE students at Sandia and UT: it was an honor sharing an office with you all during this project. Our conversations and office shenanigans are memories that I will never forget.

And finally, last but by no means least, I am thankful for my family. Mom, Dad, Ali, Jacob, and Jason - thank you for all of your love and support. I am truly lucky to have such a strong and unique family. This one is for you.

This work was partially funded by Sandia National Laboratories, which is a multi-mission laboratory managed and operated by National Technology and Engineering Solutions of Sandia, LLC., a wholly owned subsidiary of Honeywell International, Inc., for the U.S. Department of Energy's National Nuclear Security Administration under Contract DE-NA0003525.

Abstract

Long-Term Reliability Analysis of Wave Energy Converters

Jarred David Canning, M.S.E.
The University of Texas at Austin, 2017

Supervisor: Lance Manuel

Due to the highly stochastic nature of the ocean environment, offshore structures need to be designed to withstand widely varying forces without compromising performance. In particular, wave energy converters (WECs) are devices that aim to capture power from incoming waves while remaining structurally intact for a planned deployment period. The structural integrity of these WECs comes into question if the device encounters a rare and violent sea state. This study analyzes different techniques used to derive long-term loads for two wave energy devices. In addition, comparisons are made between the methods in terms of efficiency and accuracy. For one device, called Reference Model 3 (RM3), a binning scheme is utilized over all sea states to predict long-term loads using direct integration. It is found that the selected binning grid is too coarse for a fair comparison to be made to the results from another method,

the environmental contour method. For the second device, a centipod model, parametric fitting is employed to describe the metocean wave data as well as for short-term extreme response distributions obtained from WEC response simulation. The long-term response predictions from the different methods are shown to be reasonably consistent with each other in terms of accuracy and uncertainty estimates. Direct integration over all sea states and the use of Monte Carlo simulations lead to consistent prediction of rare long-term loads as long as the discretization of the metocean data (in the integration) is fine enough. Additionally, in direct integration, increasing the number of simulations around sea states with high expected loads decreases the long-term response variability and helps to yield consistent and accurate results.

Table of Contents

List of Tables

List of Figures

Chapter 1

Introduction

In order to maximize power generated from wave energy converter (WEC) devices, they must be able to sustain operation in a range of environmental conditions at the deployment site. The design of these generators and their survivability has been a challenge since the very first patents for wave energy conversion were awarded in the 1980s [12]. The prediction of possible extreme loads that a wave energy device might encounter is an important problem that engineers and WEC designers need to address. Accordingly, the reliability analysis based on computational modeling of WEC devices under all possible sea conditions is vital for assessing sustainability and performance [9]. Due to the highly variable nature of the seas, such reliability methods are probabilistic in nature and must employ statistical distributions for wave data and, because of the excessive cost of physical testing, the methods must increasingly rely on model-based simulations. Some of these methods require a very large amount of simulations to achieve accurate estimates of rare and large long-term loads; however, more efficient and less expensive alternative methods are also being considered. Guidance documents and standards [25], [18] offer recommendations on long-term load computation approaches for WECs and other marine energy structures.

This study deals with the long-term reliability analysis of two different WEC models: Reference Model 3 (RM3) and a centipod model [7]. Section 2 discusses the methods and results for RM3 and while Section 3 discusses the centipod model. Conclusions regarding the accuracy and efficiency of the reliability methods for each WEC are included.

Chapter 2

Long-Term Response of the Reference Model 3 WEC Device

Of interest in this study is the long-term response and performance of a two-body wave point absorber (Reference Model 3), which serves as a wave energy converter (WEC). In a previous study [20], the short-term uncertainty in this device's response was studied for an extreme sea state. We now focus on the assessment of the long-term response of the device where we consider all possible sea states at a site of interest. We demonstrate how simulation tools may be used to evaluate the long-term response and consider key performance parameters of the WEC device, which are the heave and surge forces on the power take-off system and the power take-off extension. We employ environmental data at a designated deployment site in Northern California. Metocean information is generated using approximately 20 years of data from this site (National Data Buoy Center site no. 46022). For various sea states, a selected significant wave height and peak period are chosen to describe representative conditions. Then, using a public-domain simulation tool (Wave Energy Converter Simulator or WEC-Sim), we generate various short-term time-domain response measure for these sea states. Distribution fits to extreme response statistics are generated for each bin that represents a cluster

of sea states using the open-source toolbox, WDRT (WEC Design Response Toolbox). Long-term distributions for each response variable of interest are estimated by weighting short-term distributions by the likelihood of the sea states; from these distributions, the 50-year response can be derived. The 50-year response is also estimated using an approximate but more efficient inverse reliability approach. Comparisons are made between the two approaches.

2.1 Introduction

In order to maximize the power generated, a wave energy converter (WEC) must be able to operate safely under various environmental conditions at the site of deployment. A reliability analysis based on modeling of the response in all relevant sea states is critical in assessing the performance and design life of a WEC [9]. This study addresses the long-term reliability analysis of the Reference Model 3 (RM3) WEC [23] at a selected site of interest. In particular, we aim to estimate the 50-year return period values for various response/load variables. We begin by describing the WEC and environmental data from the selected deployment site (NDBC 46022) [1]. We then describe the problem formulation of estimating the 50-year response using both direct integration as well as a useful and efficient first-order reliability method (FORM) [19, 31, 39]. Numerical studies and results of the analyses are presented and elaborated on for the different response variables that include the heave force on the power take-off (PTO), the surge force on the PTO, and the PTO extension.

2.2 Reference Model 3

The RM3 WEC is a two-body point absorber that consists of a floating body that oscillates along a spar cylinder with a submerged reaction plate. This device captures power via the heave motion of the float relative to the spar [23]. Although the operating conditions for this device call for several units to be deployed in an array at the selected location [23], the present study considers the response of only a single device. When deployed, multiple devices are typically arranged in an array and connected by mooring line systems [23].

Due to the power generation characteristics of the device, we consider the heave force on the PTO as one of the key variables of interest for a meaningful reliability analysis. Additionally, we examine the PTO extension as well because the mechanical design of the device must be sufficient to accommodate expected large displacements. The last response variable we study is the surge force on the PTO, which is essentially a bearing restraint force for the PTO system. This force is perpendicular to the motion of the float; hence, its response is associated more with mechanical reliability than with power production. Figure 2.1 shows schematic drawings with dimensions of the RM3 device. Various properties of the RM3 model are given in Table 2.1.

2.3 Metocean Data

We consider historical wave-related data for the selected deployment site, which is the National Data Buoy Center (NDBC) station 46022, located near Eureka, California [1]. Data sampled for this analysis were from the

period from 1996 to 2015. Pairs of significant wave height, H_s, and energy period, T_e, were obtained from the NDBC data via spectral analysis. In our device response simulations, we convert the energy period values to the spectral peak period, T_p [40]. This conversion is carried out by using the equation presented in Table A.2 of Reference [33] and by assuming that the waves follow a JONSWAP spectrum. The resulting (H_s, T_p) pairs describe the various sea states in the data. Figure 2.1 summarizes the data for this site and also shows the 50-year environmental contour. We use these observed pairs of significant wave height and peak period to help establish input parameters needed to study in the device response simulations discussed later. The site data are also used to define the 50-year environmental contour [8].

2.4 WEC Response Simulations

In order to simulate the performance of the device in different sea states, we employ the open-source simulation software, WEC-Sim [40]. This software tool takes the physical properties of any WEC device along with sea state information (to define the waves) as input and produces several performance-related output quantities, such as the response variables that are analyzed in this study. Figure 2.3 shows the RM3 model developed in Simulink using the WEC-Sim library. Each response variable is output as a time series. Representative 200-second segments of such response time series along with the sea surface elevation are shown in Figure 2.4 for a single selected sea state. Power spectral density function plots for the same sea state are displayed in

Figure 2.5. We discuss in a subsequent section how we choose to carry out 15 one-hour simulations for each selected sea state in order to gain sufficient data on extreme values. These results will be used in our long-term reliability assessment.

2.5 Extreme Response Statistics

The output time series from WEC-Sim are used with another open-source software tool, WDRT, to obtain estimates of various short-term extreme response distributions [8]. In the present study, this software tool is used to fit a Weibull distribution to the maximum response values from each simulation. Weibull fits to the short-term response data for each sea state are then used in the 50-year load prediction. The software tool is also used to establish environmental contours that define critical sea states identified using a principal components analysis (PCA) methodology [8]. These sea states enable efficient estimation of 50-year response levels using the environmental contour method that can be compared with a more rigorous procedure that involves integration of short-term response extreme distributions weighted by the likelihood of all sea states involved.

2.6 Problem Formulation

To begin, we divide the environmental (H_s, T_p) data into discrete bins. We note that most sea states are associated with low significant wave heights and short periods. While more severe sea states have the potential to cause

higher device response and load levels, they occur far less often. Both the relative likelihood and the possibility of higher response levels influence the long-term reliability of the device.

We select (H_s, T_p) bins by even discretization in both significant wave height and peak period. In this study, the significant wave height discretization is 1.5 meters and the peak period data is 3 seconds, as shown in Figure 2.6. The weight or probability of occurrence of each bin, needed in the long-term reliability computation by direct integration, is taken as the number of data in that bin divided by the total number of data. Additionally, to avoid the very low-probability areas, certain bins were not considered if the number of data in those bins was less than 20. This approximation can be relaxed and sea states in the omitted bins can be easily studied to make sure that they do not cause large WEC response levels, which might make them important even if their occurrences are rare.

For each bin, a sea state shown with an asterisk in Fig. 2.6 is selected as being representative of that bin and is used in subsequent computation for the long-term reliability assessment by the direct integration method.

2.6.1 Direct Integration

In this approach, we obtain the long-term probability distribution for any load, Y, by weighting the short-term load distributions (conditional on H_s, T_p, together denoted as $\mathbf{X}$) for the selected bin by the probability of occurrence of that bin. The theoretical and discrete forms of this computation

are as follows:

$$P_T = P(Y > y) = \int P[Y > y|\mathbf{x}] f_{\mathbf{X}}(\mathbf{x}) d\mathbf{x} \tag{2.1}$$

$$= \sum P[Y > y|\mathbf{x}] P(\mathbf{x}) \tag{2.2}$$

Here, $P(Y > y|\mathbf{x})$, obtained by WEC-Sim response simulations and WDRT Weibull fits for the representative bin, represents the (conditional) short-term load distribution for the bin and $P(\mathbf{x})$ is the weight or probability of that bin. Equation (2.2) is evaluated for any specified value of y. In this study, we are especially interested in the value of y that is the 50-year load, which occurs when the total probability computed using Eq. (2.2) using 1-hour response extremes is equal to $1/(50 \times 365.25 \times 24)$ or 2.28×10^{-6}.

2.6.2 Inverse FORM: Environmental Contour (EC) Method

An alternative long-term reliability analysis involves use of the environmental contour method. This method requires a search along a constructed 50-year environmental contour in (H_s-T_p) space for the largest median extreme response in 1 hour of the response/load, y. The 50-year environmental contour is computed using WDRT. Along this contour, 20 additional sea states were selected and simulated. Figure 2.7 shows the selected sea states along the contour used in this inverse FORM calculation (using the environmental contour method). The largest of all the median 1-hour extreme response in a bin that is intersected by the 50-year environmental contour is the 50-year

load obtained in an alternative manner to the approach used by Eq. (2.2). The environmental contour method yields only approximate 50-year loads, Y_{50}; the accuracy of these EC estimates decreases as the variability in the load, Y, increases.

2.7 Numerical Studies

2.7.1 Short-Term Load Statistics

The short-term response of the RM3 device was the subject of an earlier study by the author and collaborators [20]. Typically, time-domain response simulations are carried out in reliability analysis studies and extremes over the simulation duration are studied statistically [2]. In this study, the largest response value from each 1-hour simulation is recorded and used to define the short-term distributions. This yields 15 maximum values per bin (one from each of the 15 simulations per bin) which are then fitted with a Weibull distribution to establish the short-term load distributions. These fits are used in Eq. (2.2) to produce the direct integration solution.

Unlike direct integration, the EC method only requires the median maximum response from 15 simulations; it ignores the variability in the response conditional on the sea state wave height and period values. The EC method is approximate; it is of interest then to study the variability in the response. EC-based 50-year estimates may be greater if response variability is accounted for. A measure of the variability (quantified here as the ratio of the 84th percentile 1-hour extreme response to the median extreme response)

was determined for each sea state along the contour in Fig. 2.7. Figure 2.8 shows EC 50-year response values for the WEC heave force, surge force, and PTO extension. In each figure, the median extreme response (top) and the variability in response in each sea state (bottom) are presented.

It can be seen that the variability in each response varies considerably over the different sea states and the different response measures show contrasting degrees of variability (see the lower-half plots in the figures). The variability in response in each sea state may influence the accuracy of EC-based 50-year response predictions $Y_{(50,EC)}$. The accuracy of EC (2-D I-FORM) can be improved by using 3-D I-FORM which also includes response uncertainty. Additionally, adjustments to EC 50-year estimates can be also applied, if uncertainty is accounted for in the simulations.

Figure 2.9 summarizes the short-term probability distributions for a single sea state associated with a critical conditions for 50-year loads, where $H_s = 7.6$ m, $T_p = 12.5$ s. This figure shows the 15 1-hour heave force, surge force, and PTO extension extremes, respectively, for this sea state along with Weibull distribution fits to the data.

2.7.2 Long-term Response

Figure 2.10 shows long-term probability distributions for all three load/response variables of interest. These distributions are obtained using Eq. (2.2). The 50-year levels in each case are indicated by red circles corresponding to probability of exceedance (PoE) levels equal to 2.28×10^{-6}.

Table 2.2 compares 50-year loads based on direct integration (Eq. (2.2)) and the environmental contour (EC) method. The direct integration method appears to yield unconservative 50-year values for both heave and surge forces on the PTO. In the present study, due to the rather coarse discretization of the H_s-T_p space employed, the direct integration method's estimates themselves may be improved before drawing conclusions about the EC method's accuracy.

2.8 Conclusions

In an earlier study, the short-term response of the RM3 WEC device was studied as a function of wave height alone [20]. The present study was concerned with prediction of 50-year values for various measures of interest for the RM3 device at a site of interest. Metocean H_s-T_p data for the site were employed and using representative sea states, long-term loads were computed using both direct integration and the environmental contour (EC) method.

Planned future work will employ a finer discretization of the sea states to improve the accuracy of the direct integration method's estimates of long-term loads. Also, corrections can be applied to the EC predictions to help account for omitted response variability. As well, a greater number of simulations will be run both on and within the environmental contour so that the alternative more general 3-D inverse reliability method may provide more accurate estimates of long-term loads that go beyond the EC method and can account for response variability [21, 29].

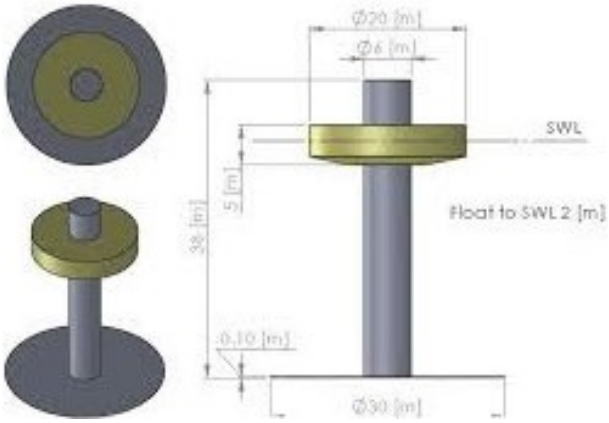

Figure 2.1: Dimensions and schematic drawings of the RM3 device [23]

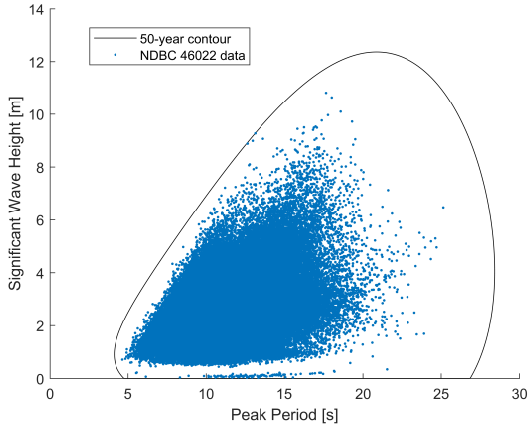

Figure 2.2: Environmental data and 50-year contour from the NDBC 46022 site [1]

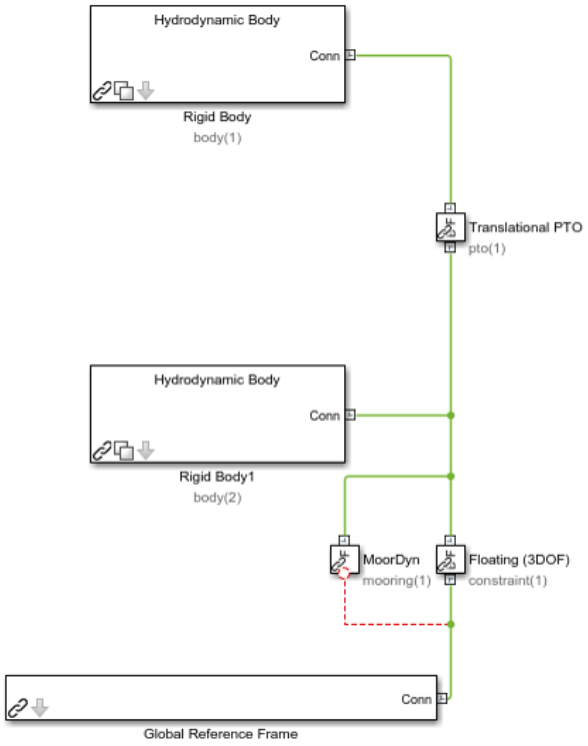

Figure 2.3: RM3 model developed using the WEC-Sim Library

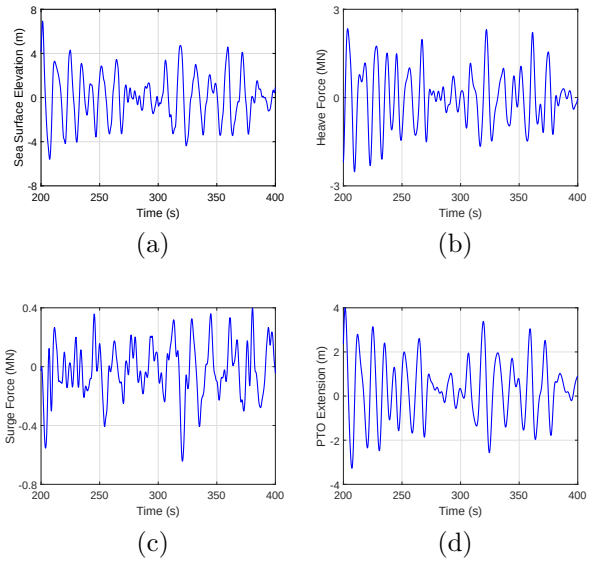

Figure 2.4: Time series plots of (a) sea surface elevation, (b) heave force, (c) surge force, and (d) PTO extension for a sea state where $H_s = 7.6$ (m), $T_p = 12.5$ (s).

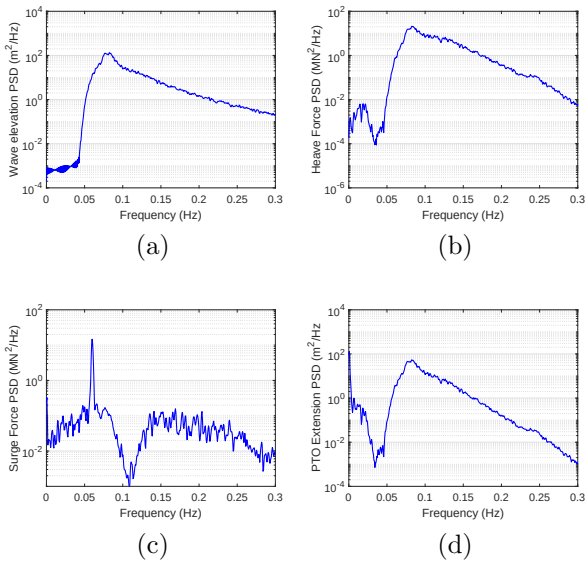

Figure 2.5: Power spectral density plots of (a) sea surface elevation, (b) heave force, (c) surge force, and (d) PTO extension for a sea state where $H_s = 7.6$ (m), $T_p = 12.5$ (s).

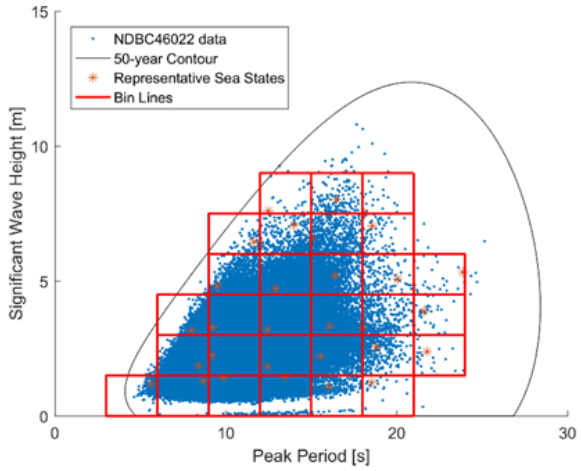

Figure 2.6: Bins selected for the study.

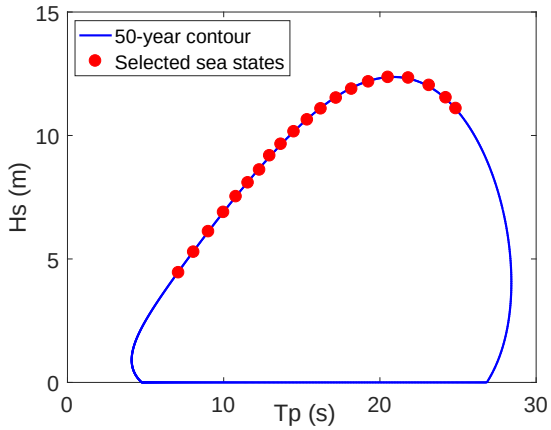

Figure 2.7: Sea states along the 50-year contour used in the environmental contour method.

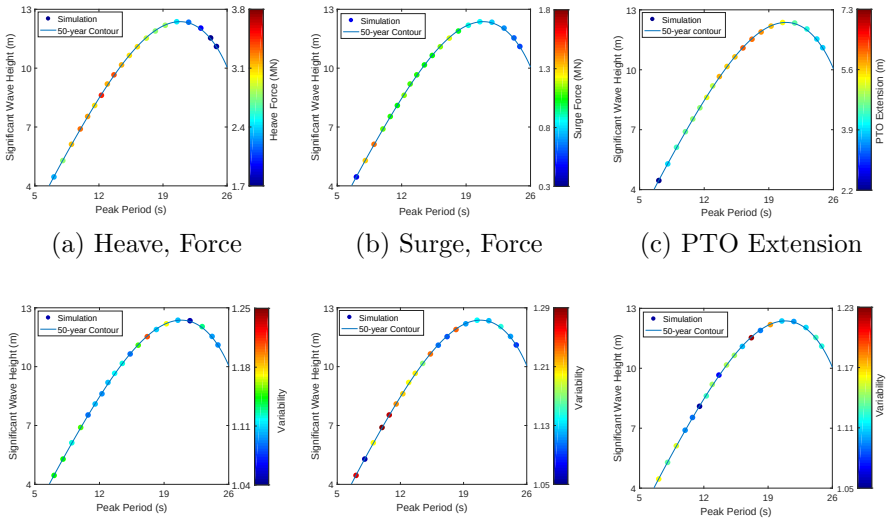

(a) Heave, Force (b) Surge, Force (c) PTO Extension

(d) Heave, Variability (e) Surge, Variability (f) PTO Extension, Variability

Figure 2.8: 50-year responses (top) and variability ratios (bottom) for heave force, surge force, and PTO extension.

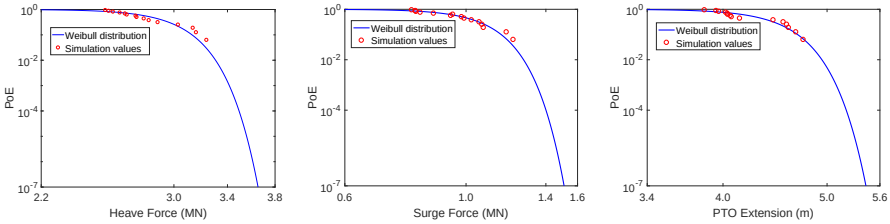

(a) (b) (c)

Figure 2.9: Short-term probability distribution fits to the 1-hour extreme response data of (a) heave force, (b) surge force, and (c) PTO extension for a sea state $H_s = 7.6$ (m), $T_p = 12.5$ (s).

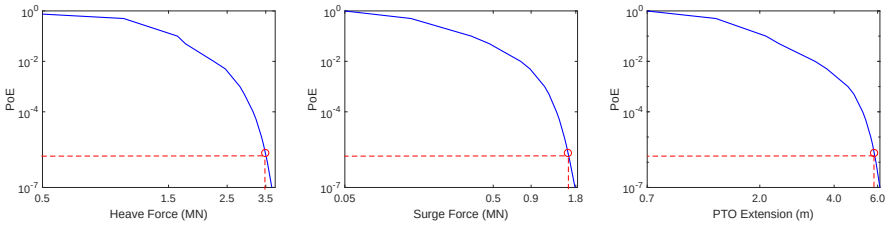

(a) (b) (c)

Figure 2.10: Long-term probability distributions for the 1-hour extreme response: (a) heave force, (b) surge force, and (c) PTO extension.

Table 2.1: RM3 Model Properties

Float Full-Scale Properties				
CG (m)	Mass (tonne)	Moment of Inertia (kg-m^2)		
0		20.9E6	0	0
0	727	0	21.3E6	4.3E3
-0.72		0	4.3E3	37.1E6
Plate Full-Scale Properties				
CG (m)	Mass (tonne)	Moment of Inertia (kg-m^2)		
0		94.4E6	0	0
0	878	0	94.4E6	2.2E5
-21.29		0	2.2E5	28.5E6

Table 2.2: Fifty-year response values based on the direct integration and EC methods

Response	Direct Integration	Environmental contour
Heave Force (MN)	3.49	3.45 (8.6 m, 12.5 s)
Surge Force (MN)	1.60	1.44 (6.1 m, 9.2 s)
PTO Extension (m)	5.82	6.11 (11.1 m, 16.7 s)

Chapter 3

Long-Term Response of the Centipod WEC Device

3.1 Centipod Model

The WEC model used in this study is a point absorber with the geometry of a centipod (shown in Fig. 3.1). The device's mass is 78,000 kg and the resting waterline is at its hemisphere. The float is an oblate spheroid with a vertical axis of symmetry, and with principal radii, r_1 equal to 4.5 meters and r_2 equal to 1.8 meters [7].

The device is connected to the ground via a power take-off (PTO) system and the motion is restricted to a single degree of freedom in the vertical direction (transverse to the direction of incoming waves). Using the boundary element method software WAMIT [37], we can estimate important hydrodynamic properties of the device. Because the device is confined to one degree of freedom in the vertical direction, our quantities of interest in this study will be the displacement (extension) and force on the PTO. The PTO force is directly related to the captured power of the WEC and the PTO extension relates to the design and fatigue of the device.

The results from three different long-term response predictions methods

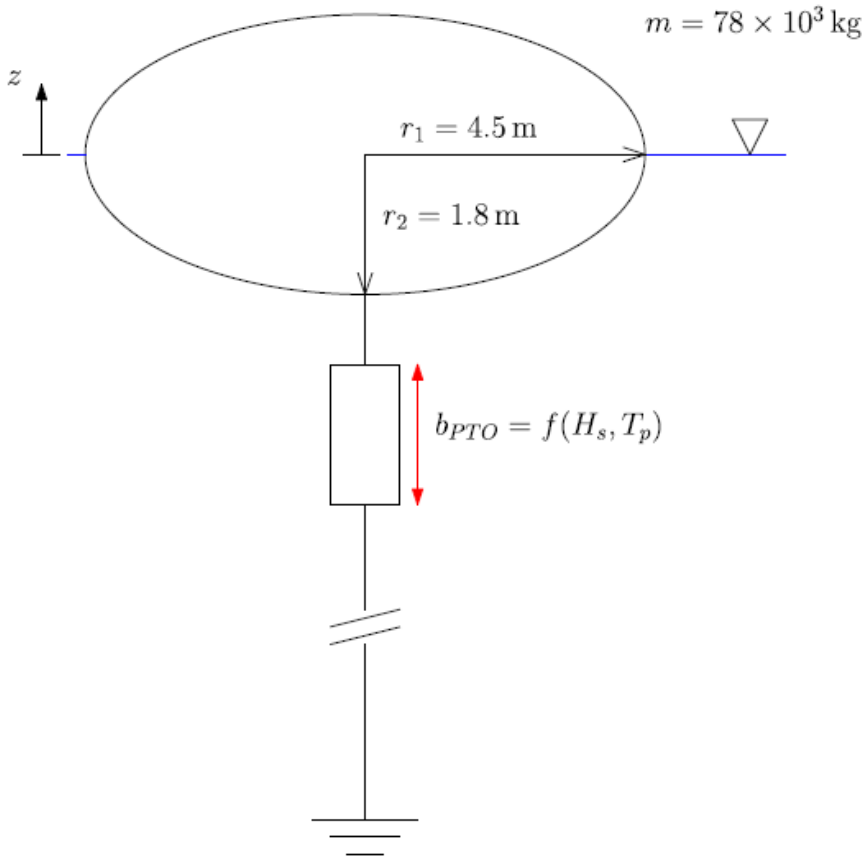

Figure 3.1: WEC model geometry and components

for our WEC model are presented later in this chapter. When comparing the values from each of the methods, it is important to note both the accuracy and the computational time associated with each method. Conclusions and discussions are included at the end.

3.2 Metocean Data

The NDBC (National Data Buoy Center) Station 46022 is located off the coast of Eureka, California and reports wave data on an hourly basis. Pairs of significant wave height, H_s, and peak wave period, T_p, were obtained from this station using WDRT [8]. The resulting data covering the period from 1996 to 2016 are presented in Fig. 3.2 [1], which contains nearly 1.5×10^5 sea state realizations. There is a large density of points from 1 m ¡ H_s ¡ 4 m and 6 s ¡ T_p ¡ 15 s, which means that these sea states occur more often than those outside of these bounds. Although these sea states are more frequent, their ability to produce large response loads is also important when assessing long-term loads.

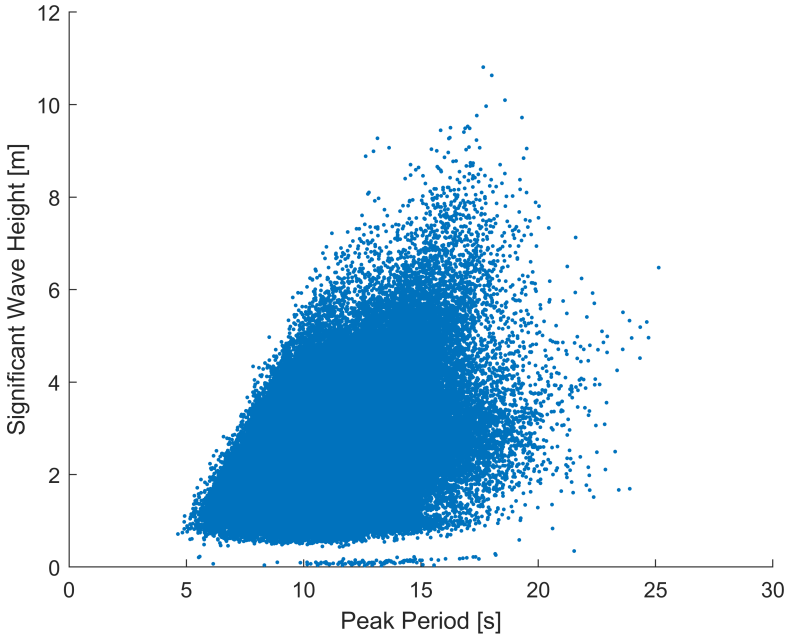

Figure 3.2: Sea states at NDBC 46022 from 1996 to 2016

For the two variables of interest, H_s and T_p, various derived statistical parameters and distributions are summarized here. In this study, parametric distributions were used to fit to the data. For the marginal distribution of H_s, a two-parameter Weibull model is used with scale factor, α, and shape factor, δ; thus, we have:

$$f_{H_s}(h) = \frac{\delta}{\alpha}\Big(\frac{h}{\alpha}\Big)^{\delta-1} \exp\Big(-\Big(\frac{h}{\alpha}\Big)^{\delta}\Big) \tag{3.1}$$

To go with the marginal distribution for H_s, a lognormal conditional distribution for T_p given H_s is also fit to the data such that the mean and standard deviation of $\ln(T_p)$ are now functions of H_s (see also Fig. 3.3); thus, we have:

$$\begin{aligned} f_{T_p|H_s}(t|h) &= \tfrac{1}{\sqrt{2\pi}\zeta(h)t} \exp\Big(-\tfrac{1}{2}\Big(\tfrac{\ln t-\lambda(h)}{\zeta(h)}\Big)^2\Big) \\ \lambda(h) &= a_1 + a_2 h + a_3 h^2 + a_4 h^3 \\ \zeta(h) &= b_1 + b_2 h + b_3 h^2 \end{aligned} \tag{3.2}$$

For discrete bins of H_s values, parameters of the conditional probability density function, $f_{T_p|H_s}(t|h)$, are also estimated by the maximum likelihood method and these estimates are then used to yield the two functions in Eq. (3.2) using ordinary least-squares regression. These regression-generated constants that define the conditional distribution parameters, as well as the α and δ parameters from the marginal H_s distribution, are presented in Table 3.1.

This parametrization of the H_s-T_p space is useful for sampling random sea states and determining environmental contours.

Table 3.1: Constants related to the Parameters for the Marginal Distribution of H_s and the Conditional Distribution of T_p (given H_s) for the NDBC 46022 Station.

α	δ	a_1	a_2	a_3	a_4	b_1	b_2	b_3
2.7528	2.264	2.3918	-0.0688	0.030	-0.0018	0.2118	-0.0053	-0.0011

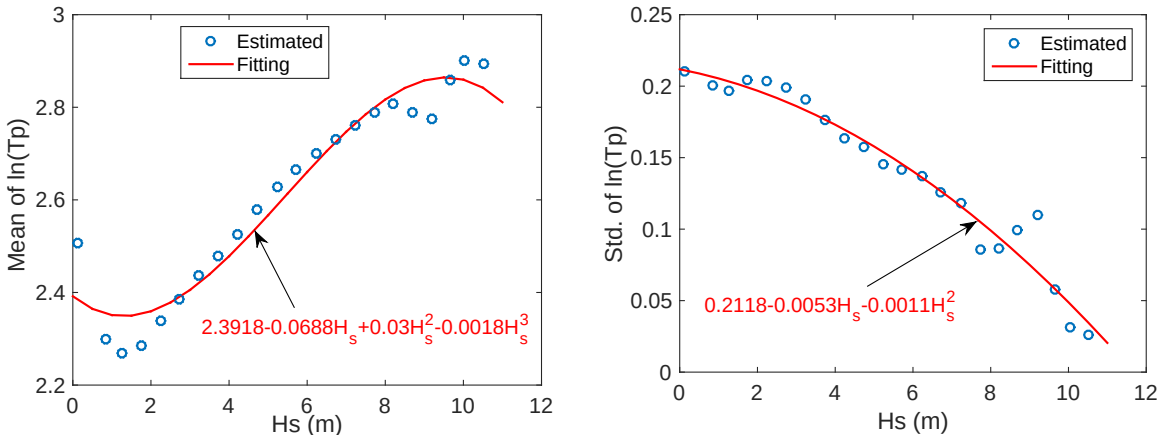

(a) (b)

Figure 3.3: Regression-based fits to (a) the conditional mean and (b) the conditional standard deviation of $\ln(T_p)$ given H_s for the NDBC 46022 station.

For our study, we will select certain sea states as well as generate random H_s and T_p combinations. We will consider the metocean conditions to be defined by a JONSWAP spectrum (Joint North Sea Wave Project) using the significant wave height, peak period, and a peakedness factor of $\gamma = 3.3$ [16]. To produce wave elevation histories in the time domain, irregular waves are simulated with amplitudes given based on the JONSWAP spectrum that are

combined with random phases [7].

3.3 WEC Response Simulations and Extreme Statistics

In order to simulate the response of the centipod for various sea conditions, a Python script developed by Sandia National Laboratories was used [7]. This script accepts the WEC properties and wave excitation information as inputs and produces several output response processes, including the quantities of interest in this study (extreme PTO motions and forces) A flow chart presented in Fig. 3.4 shows various input parameters and output processes that are related to this time-domain solver.

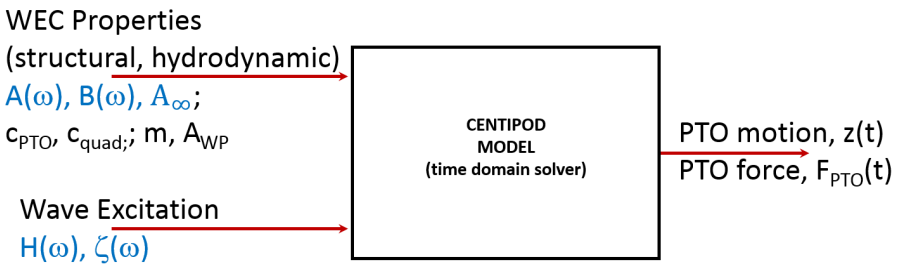

Figure 3.4: Simulation inputs and outputs for the centipod WEC model.

In Fig. 3.4, $A(\omega)$ is the added-mass frequency response function (FRF), $B(\omega)$ is the radiation damping FRF, A_∞ is the infinite-frequency added mass, c_{PTO} is the PTO damping factor, c_{quad} is the quadratic viscous damping, m is the mass of the device, and A_{WP} is the area of the water-plane. Also, $H(\omega)$ is the complex excitation FRF, and $\zeta(\omega)$ is the frequency dependent

wave spectrum. The PTO motion and force, $z(t)$ and $F_{PTO}(t)$, respectively, are the output processes of interest from the time-domain solver. The 1-hour extreme from the time series of each response will be used to establish short-term extreme values and their distributions. This methodology is used in both the long-term response prediction methods considered in this work. Figure 3.5 shows a typical 200-second portion of the response time series and wave elevation at a selected sea state. Figure 3.6 displays the power spectral density function plots for these time series in the selected sea state.

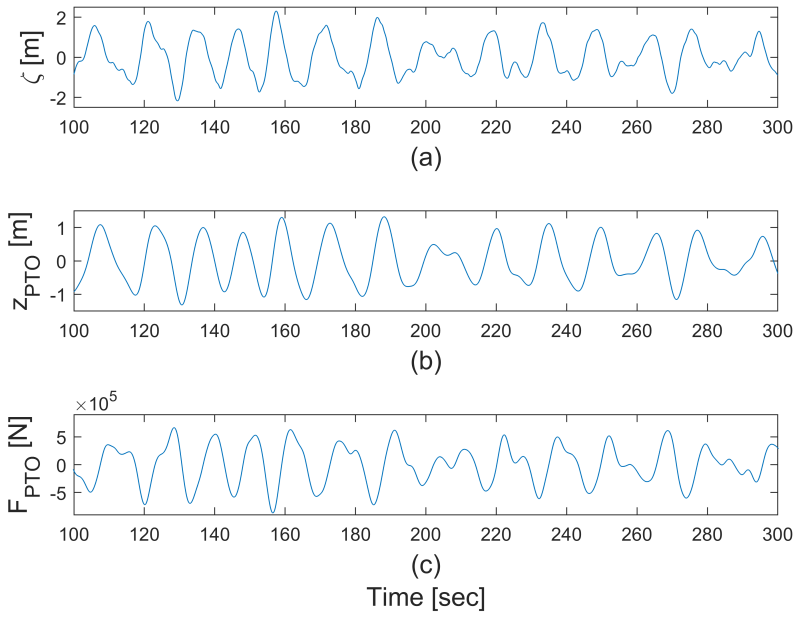

Figure 3.5: Representative time series at $H_s = 3.75$ meters, $T_p = 14.5$ seconds for a) wave elevation, b) PTO extension, and c) PTO force

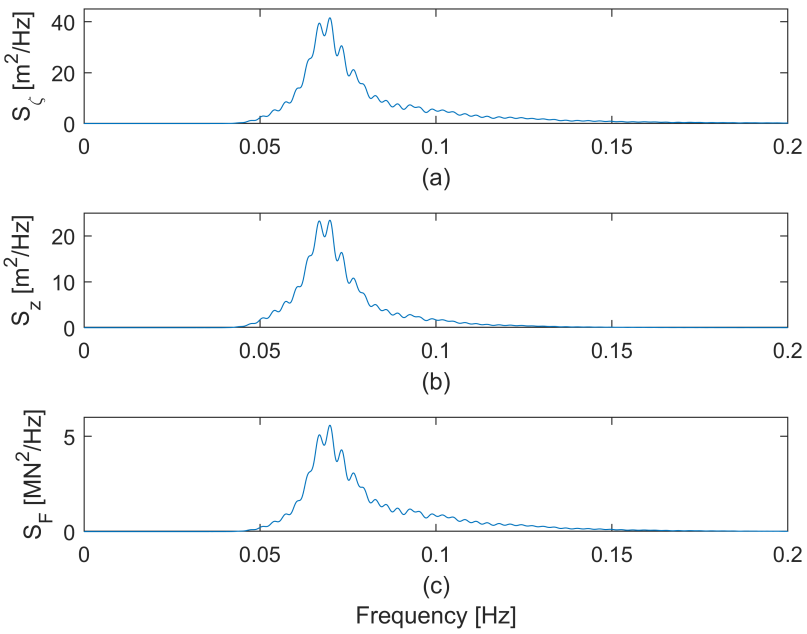

Figure 3.6: Representative power spectral density functions at $H_s = 3.75$ meters, $T_p = 14.5$ seconds for a) wave elevation, b) PTO extension, and c) PTO force.

3.4 Problem Formulation

In this study, we use two different procedures to predict long-term loads on the selected centipod WEC model and compare them with results from Monte Carlo simulation (MCS). The outline for both of these methods is to: 1) characterize the metocean data, 2) simulate the WEC model response in the derived sea states for some duration of time, and 3) extract short-term extreme loads that are then used to assess the long-term loads. For both methods, a sea state simulation duration of one hour is used. The results from these methods are given in Section 3.5 along with a brief discussion on their

implications in long-term design.

3.4.1 Direct Integration

A computationally expensive technique commonly used to predict long-term loads is direct integration. This approach integrates the short-term weighted response from a selection of sea states to estimate the long-term response. The general direct integration formulation is an application of the Law of Total Probability in the following form:

$$P_T = P(L > l) = \int_h \int_t P[L > l|(h,t)] f_{H_s,T_p}(h,t) dh dt \tag{3.3}$$

where P_T is the exceedance probability, l is a specified load level, and $f_{H_s,T_p}(h,t)$ is the joint probability function of H_s and T_p. Changing the load level l will yield different values of P_T. One can systematically change l and integrate over all relevant sea states to obtain the full long-term distribution. Conversely, if a specific load for a given exceedance probability is desired, then one can iterate Eq. (3.3) until the target probability is reached.

In this work, we generate a grid over the sea state space and select representative (H_s, T_p) pairs to simulate. We do this because full integration of the sea state space, much like Monte Carlo simulations, would require a very large number of simulations over a wide variety of sea states. To reduce the computational effort required, we use the gridding scheme shown in Fig. 3.7, where the stars indicate the representative sea states. These representative sea

states are named so because results from simulation for only these sea states will be assumed to represent the whole bin.

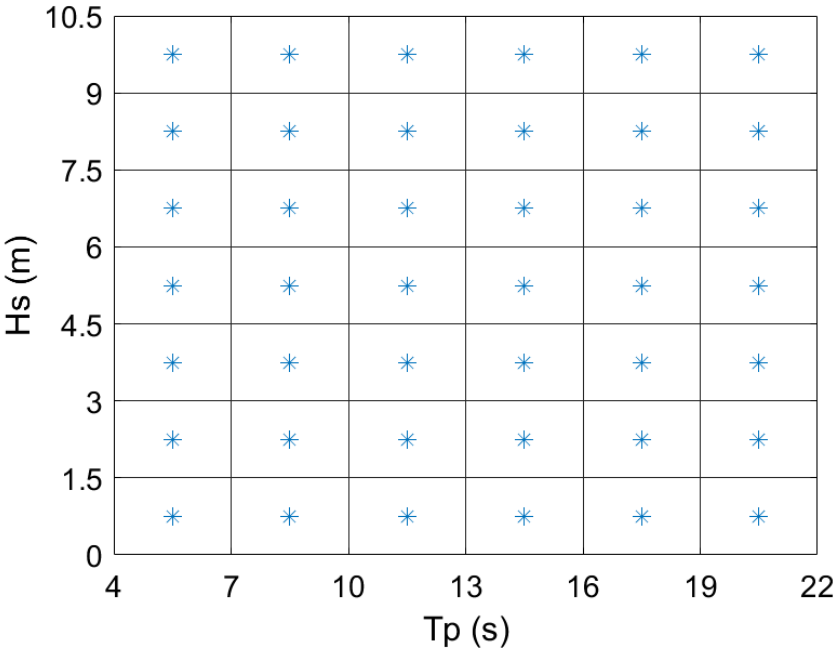

Figure 3.7: Grid used in the direct integration analysis. Starred values are the representative sea states for each bin.

Because of the gridding scheme, the double integral in Eq. (3.3) reduces to a double sum over the applicable bins:

$$P_T = P(L > l) = \sum \sum P[L > l|(h,t)] f_{H_s,T_p}(h,t) \Delta h \Delta t \qquad (3.4)$$

where Δh and Δt are the relevant bin sizes, which are assumed constant in this study.

For each representative sea state, 15 simulations were initially run with more simulations added later to obtain converged short-term distributions. From each simulation, the 1-hour extreme value from the time series was extracted. Then, the short-term extreme distribution for each bin was established by fitting a Weibull distribution to the 1-hour extreme values from each representative sea state (the Weibull CDF is given in Eq. (3.5)).

$$F_{ST}(x) = 1 - e^{-\left(\frac{x}{\alpha}\right)^{\beta}} \tag{3.5}$$

where α and β are the scale and shape parameters of the distribution, respectively. These values are obtained from the Weibull fit to the highest 50% of the 1-hour extreme values from each bin.

The joint probability for each sea state is found using the density functions given in Eqs. (3.1) and (3.2) for the representative sea states and for each bin. Performing the summation indicated in Eq. (3.4) will yield an exceedance probability associated with any load level, l. Since we are considering 50-year response values based on one-hour simulations, our target value for P_T is $1/(50 \times 365.25 \times 24) = 2.281 \times 10^{-6}$. Either by iterating Eq. (3.4) or plotting the long-term distribution, we can estimate long-term loads associated with this exceedance probability.

3.4.2 Inverse FORM: Environmental Contour Method

The simplest of the long-term prediction methods used in this study is the environmental contour method. For WEC design, contour analyses have

become increasingly popular in predicting long-term loads [5, 7, 14]. In this method, one generates a contour of sea states that is associated with a desired return period. Simulations are performed for sea states along the contour followed by a search for the maximum median response. Once this load is identified, its value and its corresponding sea state become the design load and controlling sea state. Unlike direct integration and Monte Carlo simulation, the environmental contour method doesn't rely on excessive computation. However, because only median loads are considered and because response variability is not accounted for, there is a sacrifice in accuracy with this technique compared to the other two. To account for response variability, correction factors are sometimes used with this EC method [2, 32]. In the present study, we will employ the maximum median response and add one standard deviation level to approximately count for ignored response variability.

In this study, the 50-year contour for NDBC 46022 was determined using the Rosenblatt Transformation [17, 30]. This process maps H_s and T_p into independent standard normal (Gaussian) variables U_1 and U_2 as follows:

$$\begin{aligned} U_1 &= \Phi^{-1} F_{H_s}(h) \\ U_2 &= \Phi^{-1} F_{T_p|H_s}(t|h) \end{aligned} \tag{3.6}$$

where $\Phi(\cdot)^{-1}$ is the inverse cumulative distribution function of a standard normal random variable. In the transformed space, points associated with the same probability of exceedance define a circle of radius, β, where β is defined

as:

$$\beta = -\Phi^{-1}(P_T) = -\Phi^{-1}(2.281 \times 10^{-6}) = 4.58 \tag{3.7}$$

Once the U_1 and U_2 pairs along the circle are found, we simply tranform these standard normal variables back to the physical randomv ariable space. [17]. Figure 3.8 shows the resulting Rosenblatt-based contour as well as the selected sea states for the analysis. For each of the selected sea states, 15 1-hour simulations were run and the 1-hour extreme value was extracted from each simulation. The largest of the median 1-hour extreme values from the chosen sea states is the design load.

3.5 Long-Term Response Predictions

Figures 3.9 and 3.10 show the median response levels used in the environmental contour analysis. Generally, we note that there is a increase in response level with increasing significant wave height. This suggests that the WEC model is more sensitive to changes in H_s than T_p.

The converged accuracy of the direct integration answer can be achieved in two ways: 1) by refining the grid/binning resolution; and 2) by obtaining more accurate short-term extreme distributions. To accomplish the second of these two options, additional simulations need to be run in each bin to gain a better understanding and more data for the short-term response. Figures 3.11 and 3.12 show how the direct integration results change as the number of simu-

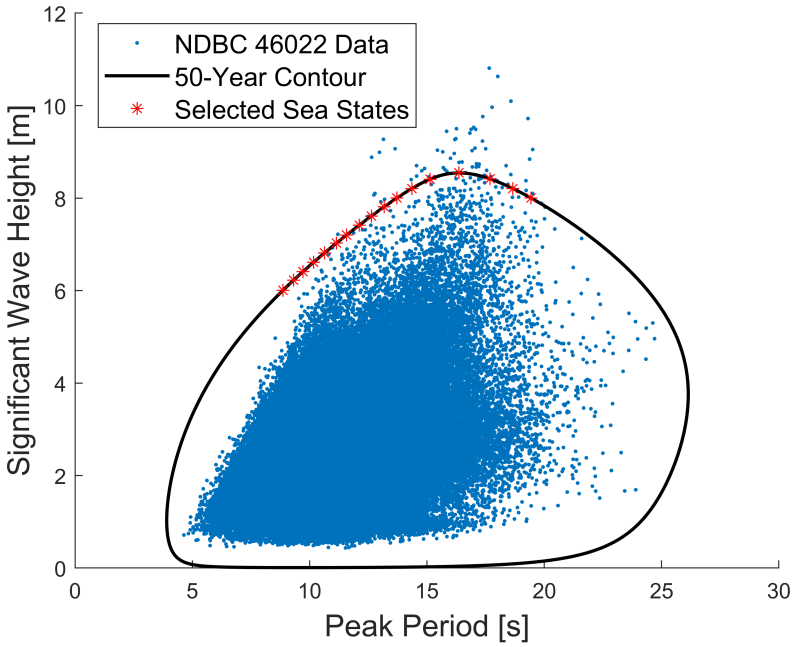

Figure 3.8: Rosenblatt contour and selected sea states based on the original metocean data

lations per sea state increases. With 30 simulations, the results appear to have converged for the selected gridding scheme. Additionally, results from Monte Carlo simulation (MCS) appear to have the same trend as the long-term distribution from direct integration, even though there are not enough simulations carried out with MCS to reach the desired probability of exceedance level. One may extrapolate the Monte Carlo results to the target probability level since the trend is evident; the direct integration results match this trend very well.

Table 3.2 compares long-term load evaluations from both of the methods (DI and EC). The addition of one standard deviation to the environmental contour value as well as the controlling sea states are also listed.

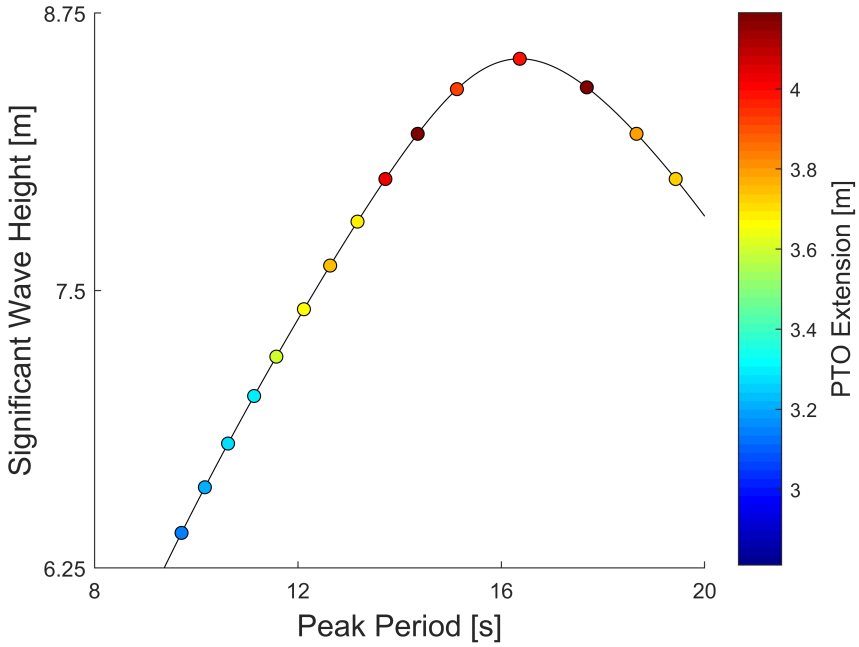

Figure 3.9: Environmental contour (EC) method values for PTO extension at the selected sea states along the 50-year contour

As one can see from Table 3.2, the long-term values from direct integration are higher than those from the environmental contour method, even with the addition of one standard deviation to the conventional EC method's prediction. We should note that direct integration is performed only over an area in the sea state space and that short-term extreme values can change depending on the load level. In the environmental contour method, only the median load is considered, which doesn't take into consideration load variability. Although seemingly more accurate, direct integration requires nearly 5 times the computational effort needed with the contour approach. The DI computational time would increase further if we used a finer gridding scheme,

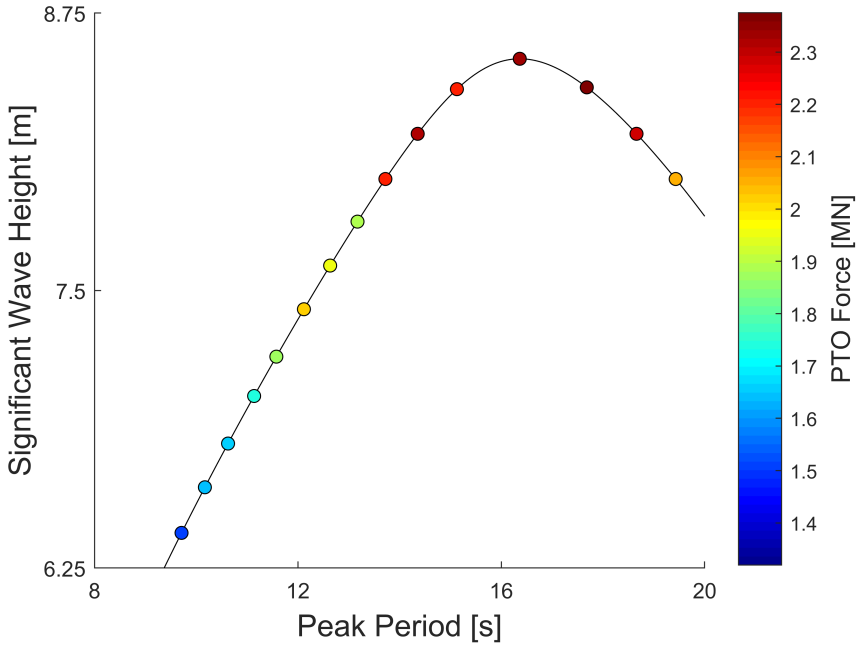

Figure 3.10: EC method values for PTO force at the selected sea states along the 50-year contour

which is discussed in the next section.

3.5.1 Finer Discretization of Bins with Direct Integration

As discussed earlier, one way to gain more accurate direct integration long-term response predictions is to employ a finer discretization of sea state bins. However, this adds computational time and costs. Instead, we note that only a subset of sea states contribute the bulk of the direct integration result. Hence, the proposed refinement is based on the fact that some sea states cannot produce large loads obtained by direct integration, even if they are associated with a high probability of occurrence. We study the product

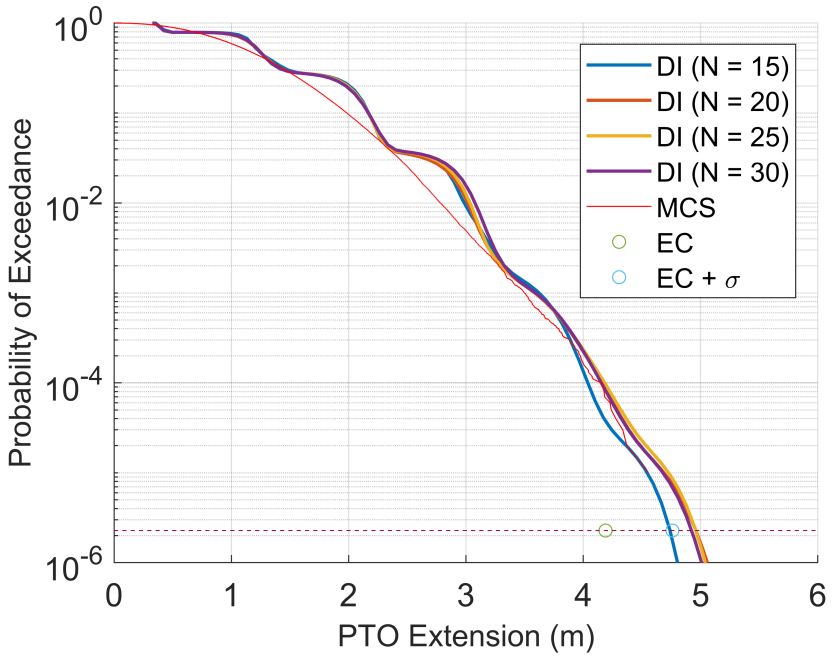

Figure 3.11: Long-term probability distribution plots for PTO extension using direct integration (DI) and Monte Carlo simulation (MCS). These results are also compared against the EC method and for the "EC plus one standard deviation" values

of the short-term extreme distribution function and the probability of bin occurrence values to gain a better understanding of which bins are important in the overall direct integration. In this manner, we concentrate bin refinement on only the most significant bins without adding an excessive number of new simulations. Figure 3.13 shows the refinement of some important bins and the resulting new representative sea states. These new smaller bins are important because the product of their short-term extreme response probability and the bin probability makes up a large portion of the overall direct integration.

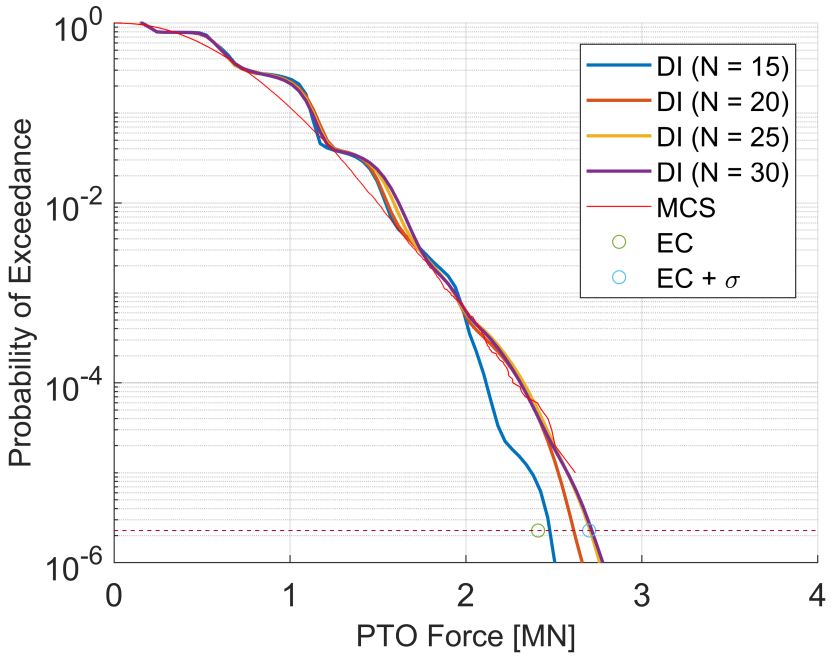

Figure 3.12: Long-term probability distribution plots for PTO force using direct integration (DI) and Monte Carlo simulation (MCS). These results are also compared against the EC method and for the "EC plus one standard deviation" values

Figures 3.14 and 3.16 show the effect of the refined binning as well as that of increasing the number of simulations.

Similar to the original binning of the H_s-T_p data, increasing the number of simulations changes the direct integration results. Long-term response results obtained with the new grid are somewhat larger than those with the original binning, as shown in Table 3.3. If an even finer grid is used, we would expect an even more accurate direct integration result than both of the previous gridding schemes.

Table 3.2: Long-term responses for each of the different methods used in this study

Response	DI	EC (+ 1 Standard Deviation)	Controlling Sea State (H_s, T_p)
PTO Extension [m]	4.92	4.19 (4.76)	(8.21 m, 14.35 s)
PTO Force [MN]	2.72	2.41 (2.70)	(8.42 m, 17.68 s)

Table 3.3: Comparison of direct integration results with a finer bin discretization scheme

Response	DI	Refined DI
PTO Extension [m]	4.92	5.40
PTO Force [MN]	2.72	2.92

3.6 Conclusions

The sustainability of a centipod WEC in rare sea states at its deployment site is crucial for the design considerations and operational efficiency of the device. A full long-term approach was carried out for two quantities of interest for the centipod: the PTO extension and force. The analysis consisted of two methods commonly used to evaluate long-term response variables along with Monte Carlo simulation used for validation. The results from these methods appear to be rational and consistent, which is expected since parametric

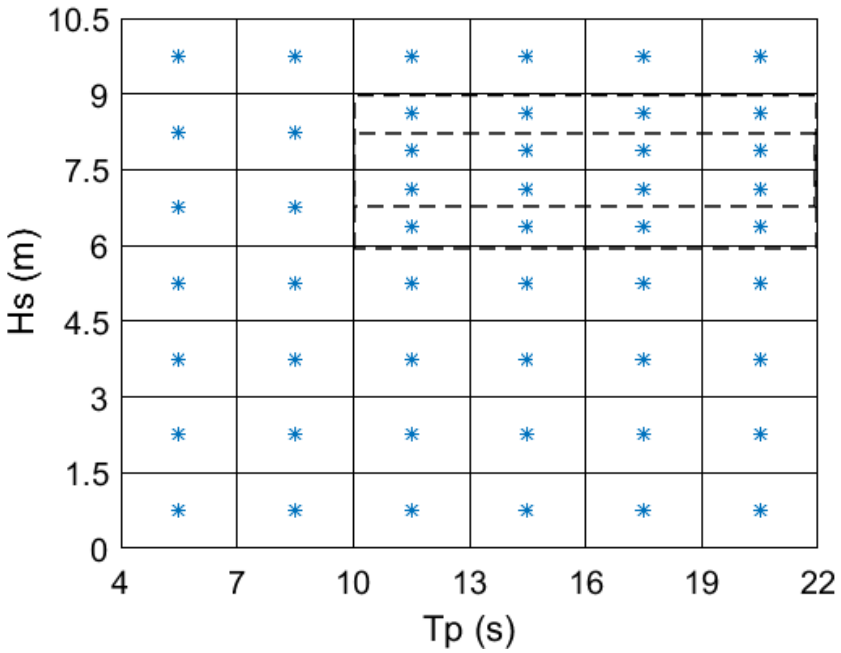

Figure 3.13: Refined binning used in the direct integration method

modeling techniques were used in all cases. Using the refined direct integration results, we predict 50-year loads for this device at the chosen deployment site to be 5.40 meters for the PTO extension and 2.92 meganewtons for the PTO force. The 50-year values from the environmental contour method for these two quantities of interest are 4.19 meters and 2.41 meganewtons, respectively.

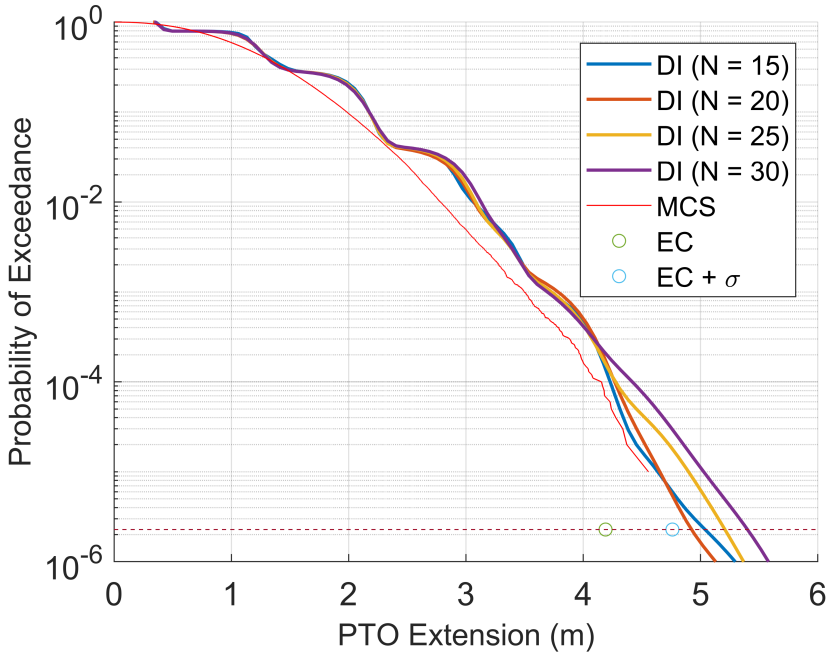

Figure 3.14: Long-term probability distribution plots for PTO extension using the refined DI grid

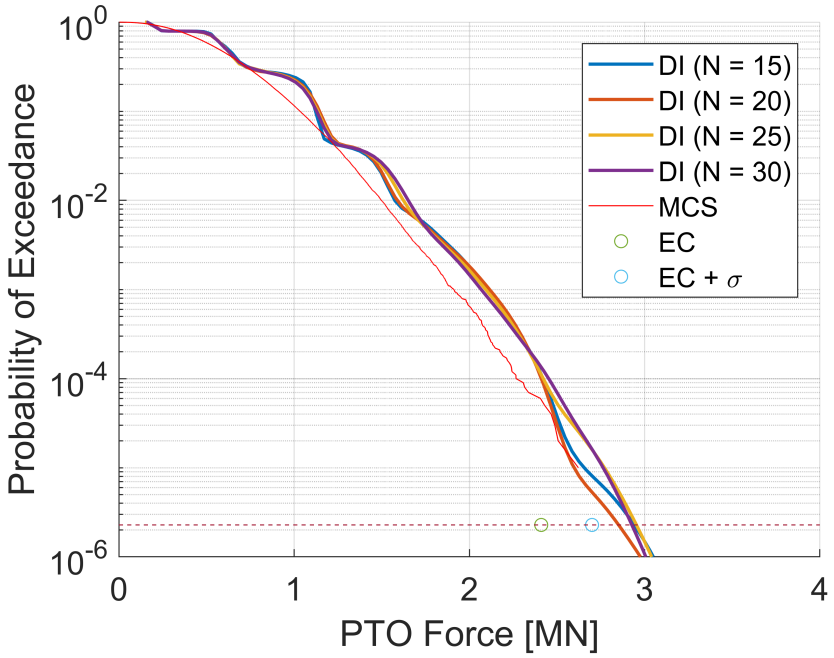

Figure 3.15: Long-term probability distribution plots for PTO force using the refined DI grid

Figure 3.16: Long-term plots for PTO force using the refined DI grid

Index

Bibliography

[1] National Data Buoy Center, Station 46022. `http://www.ndbc.noaa.gov/station_page.php?station=46022`. Accessed: 2017-12-08.

[2] P. Agarwal and L. Manuel. Simulation of offshore wind turbine response for long-term extreme load prediction. *Engineering Structures*, 31(10):2236–2246, 2009.

[3] G. Bacelli, P. Balitsky, and J. V. Ringwood. Coordinated Control of Arrays of Wave Energy Devices – Benefits Over Independent Control. *IEEE Transactions on Sustainable Energy*, 4(4):1091–1099, Oct 2013.

[4] M. Borg, L. Manuel, M. Collu, and J. Liu. Long-Term Global Performance Analysis of a Vertical-Axis Wind Turbine Supported on a Semi-Submersible Floating Platform. In *Proceedings of the 34th International Conference on Ocean, Offshore and Arctic Engineering, Newfoundland, Canada*, 2015.

[5] J. Canning, P. Nguyen, L. Manuel, and R. G. Coe. On the Long-Term Reliability Analysis of a Point Absorber Wave Energy Converter. In *Proceedings of the 36th International Conference on Ocean, Offshore and Arctic Engineering, Trondheim, Norway*, 2017.

[6] M. A. Chatzigiannakou, I. Dolguntseva, and M. Leijon. Offshore Deployments of Wave Energy Converters by Seabased Industry AB. *Journal of Marine Science and Engineering*, 5(2), 2017.

[7] R. G. Coe, C. Michelén, A. Eckert-Gallup, and C. Sallaberry. Full long-term design response analysis of a wave energy converter. *Renewable Energy*, 116:356–366, 2017.

[8] R. G. Coe, C. Michelén, A. Eckert-Gallup, Y. Yu, and J. van Rij. A Toolbox for Design-Response Analysis of Wave Energy Converters. In *Proceedings of the 4th Marine Energy Technology Symposium (METS), Washington, DC*, 2016.

[9] R. G. Coe and V. S. Neary. Review of Methods for Modeling Wave Energy Converter Survival in Extreme Sea States. In *Proceedings of the 2nd Marine Energy Technology Symposium, Seattle, Washington*, 2014.

[10] W. E. Cummins. *The Impulse Response Function and Ship Motions*. Tech. Rep. DTNSDRC 1661, Department of the Navy, David Taylor Model Basin, Bethesda, MD, 1962.

[11] National Data Buoy Center. How are significant wave height, dominant period, average period, and wave steepness calculated? NOAA-NDBC. `http://www.ndbc.noaa.gov/wavecalc.shtml`. Accessed: 2017-12-08.

[12] A. F. de O. Falcão. Wave energy utilization: A review of the technologies. *Renewable and Sustainable Energy Reviews*, 14:899–918, 2010.

[13] O. Ditlevsen and H. O. Madsen. *Structural Reliability Methods.* John Wiley and Sons Ltd, 1996.

[14] A. C. Eckert-Gallup, C. J. Sallaberry, A. R. Dallman, and V. S. Neary. *Modified Inverse First Order Reliability Method (I-FORM) for Predicting Extreme Sea States.* Technical Report SAND2014-17550, Sandia National Laboratories, 2014.

[15] J. Falnes. *Ocean Waves and Oscillating Systems.* Cambridge University Press, Cambridge; New York, 2002.

[16] Y. Goda. A Review on Statistical Interpretation of Wave Data. *Report of the Port and Harbour Research Institute*, 18(1):5–32, 1979.

[17] S. Haver and S. R. Winterstein. Environmental contour lines: A method for estimating long term extremes by a short term analysis. 116, 01 2008.

[18] IEC. *Marine Energy - Wave, Tidal and Other Water Current Converters - Part 2: Design Requirements for Marine Energy Systems.* August 2016.

[19] H. O. Madsen, S. Krenk, and N. C. Lind. *Methods of structural safety.* Courier Corporation, 2006.

[20] L. Manuel, J. Canning, R. G. Coe, and C. Michelén. On the Short-Term Uncertainty in Performance of a Point Absorber Wave Energy Converter. In *Proceedings of the 4th Marine Energy Technology Symposium (METS), Washington, DC*, 2016.

[21] L. Manuel and A. Sultania. Long-term loads and motions for a spar buoy-supported floating offshore wind turbine. In *52nd AIAA Structures, Structural Dynamics and Materials Conference*, 2011.

[22] C. Michelén and R. Coe. Comparison of Methods for Estimating Short-Term Extreme Response of Wave Energy Converters. In *OCEANS 2015 - MTS/IEEE Washington*, pages 1–6, Oct 2015.

[23] V. S. Neary, M. Lawson, M. Previsic, A. Copping, K. C. Hallett, A. LaBonte, J. Rieks, and D. Murray. Methodology for design and economic analysis of marine energy conversion (MEC) technologies. In *Marine Energy Technology Symposium*, 2014.

[24] V. S. Neary, M. Previsic, R. A. Jepsen, M. J. Lawson, Y. Yu, A. E. Copping, A. A. Fontaine, K. C. Hallett, and D. K. Murray. *Methodology for Design and Economic Analysis of Marine Energy Conversion (MEC) Technologies*. Technical Report SAND2014-9040, Sandia National Laboratories, 2014.

[25] NORSOK. *Actions and Action Effects, NORSOK Standard N-003, Ed. 2*. September 2007.

[26] J. A. Oskamp and H. T. Özkan-Haller. Power calculations for a passively tuned point absorber wave energy converter on the Oregon coast. *Renewable Energy*, 45:72–77, 2012.

[27] T. Perez and T. I. Fossen. Time- vs. Frequency-Domain Identification of Parametric Radiation Force Models for Marine Structures at Zero Speed. *Modeling, Identification and Control*, 29(1):1–19, 2008.

[28] E. Quon, A. Platt, Y. Yu, and M. Lawson. Application of the Most Likely Extreme Response Method for Wave Energy Converters. In *Proceedings of the 35th International Conference on Ocean, Offshore and Arctic Engineering, Busan, South Korea*, 2016.

[29] E. A. Rendon and L. Manuel. Long-Term Loads for a Monopile-Supported Offshore Wind Turbine. *Wind Energy*, 17(2):209–223, 2014.

[30] M. Rosenblatt. Remarks on a multivariate transformation. *The annals of mathematical statistics*, 23(3):470–472, 1952.

[31] K. Saranyasoontorn and L. Manuel. A comparison of wind turbine design loads in different environments using inverse reliability techniques. *Transactions of the ASME, Journal of Solar Energy Engineering*, 126(4):1060–1068, 2004.

[32] K. Saranyasoontorn and L. Manuel. Design Loads for Wind Turbines Using the Environmental Contour Method. *Journal of Solar Energy Engineering*, 128(4):554–561, 2006.

[33] C. T. Stansberg, G. Contento, S. W. Hong, M. Irani, S. Ishida, and R. Mercier. The specialist committee on waves final report and recom-

mendations to the 23rd ittc. In *Proceedings of the 23rd ITTC*, volume 2, pages 505–551. 2002.

[34] C. T. Stansberg, G. Contento, S. W. Hong, M. Irani, S. Ishida, R. Mercier, Y. Wang, J. Wolfram, J. Chaplin, and D. Kriebel. The Specialist Committee on Waves: Final Report and Recommendations to the 23rd ITTC. In *Proceedings of the 23rd International Towing Tank Conference, Venice, Italy*, 2002.

[35] A. Sultania. Reliability Analysis of a Spar Buoy-Supported Floating Offshore Wind Turbine. Master's thesis, University of Texas at Austin, 2010.

[36] Det Norske Veritas. Recommended Practice: Environmental Conditions and Environmental Loads, DNV-RP-C205. 2010.

[37] WAMIT. WAMIT User Manual, Version 7, 2012.

[38] F. Wendt, Y. Yu, K. Nielsen, and J. Hoffman. International Energy Agency Ocean Energy Systems Task 10 Wave Energy Converter Modeling Verification and Validation. In *Proceedings of the 12th European Wave and Tidal Conference, Cork, Ireland*, 2017.

[39] S. R. Winterstein, T. C. Ude, C. A. Cornell, P. Bjerager, and S. Haver. Environmental Parameters for Extreme Response: Inverse FORM with Omission Factors. In *Proceedings, ICOSSAR-93, Innsbruck, Austria*, 1993.

[40] Y. Yu, M. Lawson, K. Ruehl, and C. Michelén. Development and Demonstration of the WEC-Sim Wave Energy Converter Simulation Tool. In *Proceedings of the 23rd International Towing Tank Conference, Venice, Italy*, 2002.

Vita

Jarred David Canning was born in Austin, Texas. After completing his work at James Bowie High School, Austin, Texas, in 2013, he entered the University of Texas at Austin. He received the degree of Bachelor of Science from the University of Texas at Austin in May 2016. During the summers of 2016 and 2017, he interned at Sandia National Laboratories in Albuquerque, New Mexico. In August, 2016, he entered the Graduate School at the University of Texas at Austin.

Email Address: jcanning14@utexas.edu

This manuscript was typed by the author.

This thesis was typeset with LaTeX[†] by the author.

[†]LaTeX is a document preparation system developed by Leslie Lamport as a special version of Donald Knuth's TeX Program.